Portable low-cost set-up for outdoor implementation of dynamic speckle technique

Mikhail Levchenko*[a,b], Elena Stoykova[a], Keehoon Hong[c], Joongki Park[c]
[a]Institute of Optical Materials and Technologies, Bulgarian Academy of Sciences, Acad. Georgi Bonchev Str., Bl.109, 1113 Sofia, Bulgaria; [b]Technical University of Berlin, 17th of June Street, 135, 10623, Berlin, Germany; [c]Electronics and Telecommunications Research Institute, 218 Gajeong-ro, Yuseong-gu, Daejeon, 34129, Republic of Korea

ABSTRACT

Dynamic speckle technique (DST) is based on speckle formation on the surface of objects illuminated with coherent light. Temporal speckle intensity fluctuations depend on the speed of micro-changes ongoing within the controlled objects. The DST visualizes as a set of 2D activity maps the temporal change of spatial speed distributions. In general, the DST set-up comprises components as a laser source with the required optics, vibration-isolated table, high-resolution camera and computer for data storage and image processing. Such set-ups are stationary, massive and relatively expensive, which decreases the number of possible DST biological or industrial applications. In this paper we propose a miniature portable device, based on a low-cost laser attached to a smartphone, and checked its efficiency under the field conditions. A strong argument for using a portable set-up is the fact that the absolute values of the speckle intensity are not needed to construct a reliable activity map. We proved this conclusion by numerical simulation of DST in noisy environment. We studied speckle patterns captured with a smartphone's camera. A personal computer (PC) was used for postprocessing of speckle images. We conducted four sets of experiments. The raw data were recorded on the PC while the smartphone was connected as i) IP-camera and ii) USB-camera. In the third experiment, speckle images were captured and stored in the smartphone's memory. Data were transferred to the PC after the end of recording. To obtain ground truth activity maps, we repeated the experiment with the same object under laboratory conditions.

Keywords: dynamic speckle, speckle, image processing

1. INTRODUCTION

Dynamic speckle technique (DST) is a method based on statistical processing of speckle patterns formed on surface of objects illuminated with a laser beam. The main goal is to estimate speed of the processes which cause changes of speckle intensity data. Some of dynamic speckle imaging applications are: monitoring of blood flow in human tissues[1-3], analysis of seeds viability[4,5], detection of plant growth[6] and chemical contamination of leaves[7], penetration of cosmetic ingredients in human skin[8], study of ear biometrics[9], bacterial response[10] and animal reproduction[11], food quality assessment[12,13] and observation of a drying process[14]. Speckle formation strongly depends on micro changes in topography and refractive index, and this makes DST a highly sensitive tool for evaluation of the speed of processes due to its direct impact on speckle intensity fluctuations in time. For the speed of processes representation, a 2D map is built which is computed from a sequence of correlated in time speckle images. The map is called an activity map as it shows instant picture of areas with faster or slower speed changes on the object surface.

Most of laboratory DST experiments are conducted in special environment with application of a vibration isolated table, a high-end camera, a high-quality laser and a beam expander. This makes impossible application of the method under field conditions. In addition, not every company can afford the use of expensive equipment. In this paper, we propose a portable device with a low-cost laser attached to a smartphone. Such a portable setup makes the DST method available to anyone. Usage of a portable setup is possible because the absolute speckle intensities are not needed for a reliable output of the measurement. We checked efficiency of the outdoor DST implementation by numerical simulation in noisy environment. We conducted the following experiments: recording of a raw data on the personal computer (PC) with the smartphone connected as IP-camera or USB-camera and capture and storage of images in the smartphone's memory with data transfer to the PC. For comparison, experiment with the same object under laboratory conditions were carried out.

2. PORTABLE DEVICE DESIGN AND DEVELOPMENT

A portable DST device allows to switch from laboratory experiments conducted with vibration isolation in a darkened room to field conditions when only a smartphone, a small laser and a tripod are needed. Figure 1 illustrates advantages of using a portable device instead of bulky and expensive equipment used for laboratory experiments. Design and development of the proposed portable device consist of two stages, which must be coordinated with each other. At the first stage, electronic parts are chosen ~~so they have~~ to correspond to the dimensions of the device housing. Since the goal is to develop a portable laser device which could be attached to a smartphone, the housing has to be small to fit on the back surface of the latter.

In case of a stationary laboratory experimental setup shown in Fig.1(a), dimensions of the laser are not of particular importance. In contrast, when designing a portable laser for DST, size and weight of the housing is one of the most important parameters to be chosen.

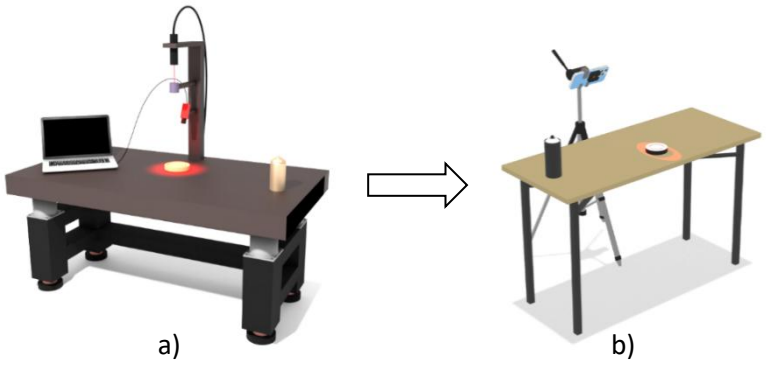

Figure 1. Stationary laboratory dynamic speckle setup (a); proposed portable DST setup (b)

The dimensions of the developed laser housing are 43 mm × 41 mm ×18 mm. For the experiment, we used ready-to-use electrical PCBs, hence their size was not optimal for the developed specific laser case. The dimensions of a manufactured version of the device could be reduced more. The functional scheme of the device is shown in Fig. 2. A laser emits at wavelength 635 nm, with power of 5 mW and 5V voltage. It is supplied with 3.7V Li-Po battery with voltage stabilized using a DC-DC converter. The battery can be charged via USB-C port with input voltage 5 V which allows to use mobile phone adaptor for charging. By pressing a switcher button, the laser may be turned on and off.

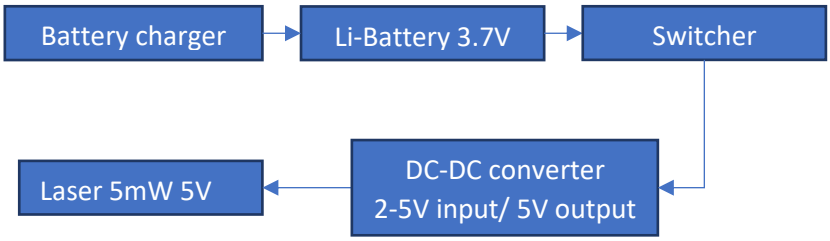

Figure 2. Functional scheme of the portable laser

At the next stage, we developed a 3D model of the laser housing. It consists of the main part for electrical components (Fig. 3a) and the cover (Fig. 3b). As it has been mentioned earlier, the size of the laser housing can be reduced in case of own PCB tracing. The final version of ready-to-use laser is shown in Fig. 3c.

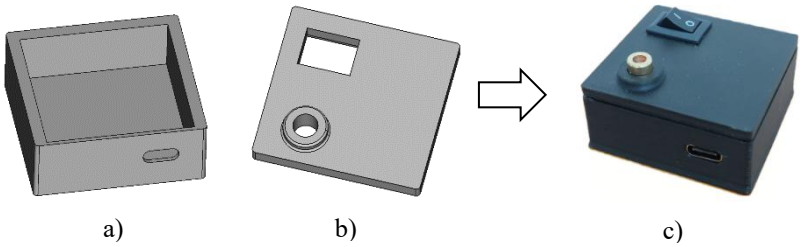

Figure 3. 3D model of the electrical components housing (a); 3D model of the hosing cover (b); Laser device (c).

In our experiment, the developed device for simplicity was attached to a smartphone's case with a double-sided tape. For further improvement, the laser housing can be developed in such a way ~~that it would~~ as to serve simultaneously as smartphone's protection case and space where the electric components are installed.

3. SIMULATION

Usage of a portable DST device means presence of environmental noise which may hamper reliable evaluation of regions of different activity across the object. To prove efficiency of using a portable device, we simulated implementation of intensity-based pointwise DST. A sequence of correlated in time images of speckle patterns of size $N_x \times N_y$ pixels at a pixel interval, Δ, are captured by an optical sensor at the time interval, Δt, between consecutive images. Pointwise processing means that a temporal sequences of intensity values, $I_{kl,i} \equiv I(k\Delta, l\Delta, i\Delta t), i = 1..N$, is formed for each pixel $(k,l) \equiv (k\Delta, l\Delta), k = 1..N_x, l = 1..N_y$ from N recorded images. The intensity values are integers in the interval from 0 to 255 for 8-bit encoded images. The formed sequences are processed by different correlation-based algorithms which give estimates related to the temporal correlation radius $\tau_c(k,l)$ of intensity fluctuations at a given object point or pixel. The contour maps of estimates visualize activity across the object within the averaging interval, $T = N\Delta t$. The estimates strongly fluctuate from point to point. The narrower the spread of fluctuations, the better the map contrast. For the pointwise DST, the averaging interval $T = N\Delta t$ can be larger or less than $\tau_c(k,l)$ at a certain pixel.

The laser beam creates a speckle pattern at wavelength, λ. Let's assume normal random shift of the scattering centers with respect to the object surface. We accept independence of the amplitude and the phase of light from a given center and mutual independence of the amplitudes and phases of the other scattering centers. No temporal change in reflectivity occurs across the object during the measurement. The phase change related to the shift of a scattering center is normally distributed at each point. The phase change, $\Delta\varphi_m^{kl}$, at point $(k\Delta, l\Delta)$ for a time lag $\tau = m\Delta t, m = 1,2...N_\tau < N$ leads to a normalized correlation function $\rho_{kl}(\tau = m\Delta t) = \exp\left(-\sigma^2\left\{\Delta\varphi_m^{kl}\right\}\right)$, where $\sigma^2\left\{\Delta\varphi_m^{kl}\right\}$ is the variance of the phase change. We used for $\rho_{kl}(\tau = m\Delta t)$ the model $\rho_{kl}(\tau) = \exp\left[-\tau/\tau_c(k,l)\right]$ to describe a drying process. The following formula is obtained for the standard deviation of the phase change, $\sigma\left\{\Delta\varphi_{m=1}^{kl}\right\} = \sqrt{\Delta t/\tau_c(k,l)}$.

Delta-correlated in space random phases $\varphi(k\delta, l\delta, i\Delta t), k = 1..2N_x, l = 1..2N_y, i = 1..N$ are generated on the object surface at a spatial step $\delta = \Delta/2$ from a 2D array of phase values uniformly distributed from 0 to 2π using the relation $\varphi(k\delta, l\delta, i\Delta t) = \varphi[k\delta, l\delta, (i-1))\Delta t] + \chi_{kl,i}\sqrt{\Delta t/\tau_c(k,l)}$ where $\chi_{k,li}$ is a random number with standard normal distribution with zero mean and variance equal to 1, $k = 1..2N_x, l = 1..2N_y, i = 1..N$. When no vibration isolation is used, phase noise is added at all moments $i\Delta t, i = 1..N$ starting from $i \geq 2$. We assume independent noisy fluctuations at the object points with the same probability distribution at all points and the same temporal correlation radius, τ_{noise}. The standard deviation of the environmental phase fluctuations was given by $\sigma_{noise} = \alpha\sqrt{\Delta t/\tau_{noise}}$ where parameter α is less than 1. The complex amplitude on the object surface for intensity distribution $I_0(k\delta, l\delta)$ of the laser beam is $U_S = \sqrt{I_0(k\delta, l\delta)}\exp\{-j[\varphi(k\delta, l\delta, i\Delta t) + \theta_{kli}\sigma_{noise}]\}$, where j is the imaginary unit, $\theta_{kl,i}$ is a random number with standard normal distribution with zero mean and variance equal to 1. The spatial intensity distribution $I_0(k\delta, l\delta)$ of the laser beam is given by real numbers. The complex amplitude of the light field on the sensor aperture is $U_{cam} = FT^{-1}\{H \cdot FT\{U_S\}\}$ where $FT\{\cdot\}$ is Fourier transform and H is a *circ* function in the Fourier domain with a cut-off frequency equal to $N_x\delta D/(2\lambda f)$, where D and f are the diameter and the focal distance of the sensor objective and $N_x = N_y$. Integration of speckle by the camera pixels was done through summation of values $|U_{cam}|^2$ in a window of size 2×2 pixels. The exposure interval was much shorter than the interval Δt.

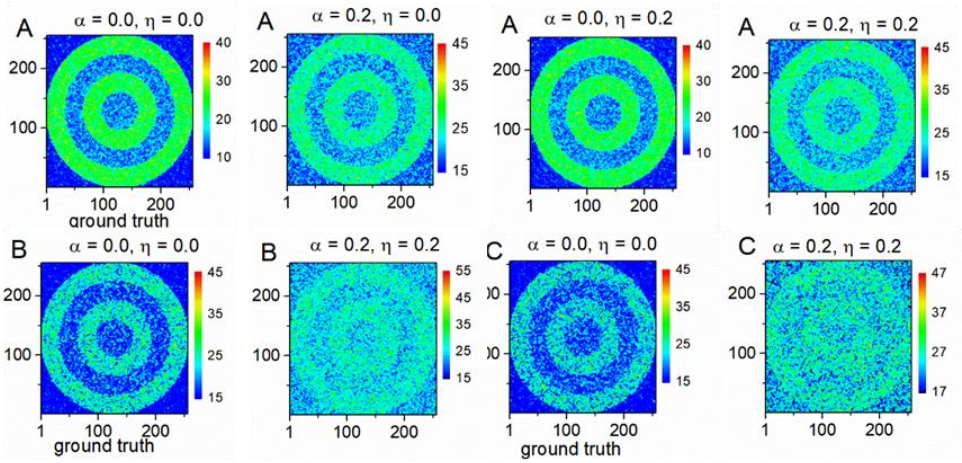

Figure 4. Activity maps as 2D distributions of estimate (1) at environmental noise for uniform illumination at wavelength 635 nm and $N = 200$, image size 256×256 pixels; A: the temporal correlation radii are 10 Δt and 40 Δt, B: the radii are 15 Δt and 40 Δt, C: the radii are 20 Δt and 40 Δt; the time lag is equal to the smaller temporal correlation radius.

We simulated the shot noise due to photons at the laser wavelength and the noise due to quantization at encoding the signal as 8-bit images. We included also the shot noise due to ambient light entering the sensor aperture at the wavelengths within the curve of spectral sensitivity of the camera in the case of the outdoor measurement. We assumed that i) the average number of signal photons within the exposure interval at the laser wavelength was $N_{ph}(l,k)$; ii) the maximum average number of signal photons was $N_{\max}$; iii) the equivalent average number of photons, $N_{al} = \eta N_{\max}$, due to ambient light was the same for all pixels with η less than 1. The shot noise was randomly generated according a Poisson distribution with average and variance equal to $N_t = N_{ph}(l,k) + N_{al}$. The camera dynamic range covered a signal equivalent to $N_{\max}(1+\eta) + \sqrt{N_{\max}(1+\eta)}$. The simulated raw data were 8-bit encoded.

We simulated noisy capture of speckle patterns for a specially designed circular object. It is composed from annular regions with alternating from the outer region to the center of the object small and large radii of temporal correlation of intensity fluctuations. This synthetic object was chosen to correspond to the object produced by a 3D printer for the experiments described below. In the experiment, the object was covered by paint. To simulate a larger correlation radius, two of the object's regions represent cut-outs with depth 3 mm below the surface that contain more paint that the flat surface and show slower evaporation process. We considered the case of uniform illumination and applied the so called modified structure function (MSF) to estimate activity:

$$S(k,l,m) = \frac{1}{(N-m)} \sum_{i=1}^{N-m} \left| I_{kl,i} - I_{kl,i+m} \right| \qquad (1)$$

This estimate increases with the rise of activity and is characterized with good sensitivity. The sensitivity of the algorithm is of vital importance for processing data captured in noisy environment. Figure 4 shows results of the simulation for 3 cases of activity distribution: i) case A with temporal correlation radii equal to 10 Δt and 40 Δt, ii) case B with radii 15 Δt and 40 Δt, and iii) case C with radii 20 Δt and 40 Δt; the time lag is equal to the smaller temporal correlation radius, wavelength is 635 nm, the number of processed images is N=200, image size is 256×256 pixels. The background region is characterized with temporal correlation radius equal to100 Δt. We especially chose high values of the parameters characterizing contribution of both vibration and shot noise due to ambient light. As is seen, both types of noise increase intensity fluctuations in the background region as well as in the other regions. The impact of the vibration phase noise is more strongly expressed. As a ground truth map, we consider the map obtained under laboratory conditions with experiments conducted with vibration isolation and in a darkened room. Despite the fluctuations induced by the noise, different activity regions are clearly seen. However, the contrast of the noisy map is strongly decreasing when the difference in activity between the regions becomes smaller.

4. EXPERIMENTAL RESULTS

For experimental verification, we captured speckle images of a cylindrical object with round cut-outs (Fig.5) that was covered with white paint Tamiya Mini X-2. The diameter of the cylinder is 50 mm and the height is 10 mm. The diameters of the walls of the annular external cutout are 40 mm and 30 mm. The diameter of the central cutout is 18 mm. The depth of the cut-outs is 3 mm. In the first experiment, we covered the object with paint and

illuminated its surface by a stationary laboratory green laser with wavelength 535 nm. During paint drying, speckle images were captured with the BASLER acA4096-30um camera. Resolution of the images is 4096 x 2168. We consider the captured in laboratory ~~data~~ images as the ground truth ~~ones~~. Next three sets of experiments were conducted with portable laser and the smartphone. Speckle images were captured with the Xiaomi Mi 9T which was connected to PC as i) IP-camera and ii) USB-camera. Finally, in the last set of experiments, the speckle images were captured and stored in smartphone's memory. Data were transferred to the PC after the end of the recording. In all smartphone experiments, images were captured with resolution 1920×1080 and 3840×2160. Duration of each recording was 10 minutes. The time interval between captured speckle images in all experiments was 300 ms. What about the exposure time?

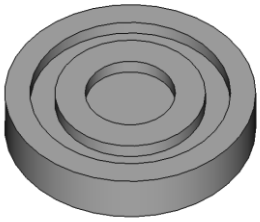

Figure 5. 3D-model of the test object

4.1 Speckle images captured with the BASLER camera

BASLER acA4096-30um camera captures grayscale images. Below (Fig. 6), an example of the ground truth cropped speckle image is shown. Average intensity was chosen by building histograms in **Pylon** software provided with the camera.

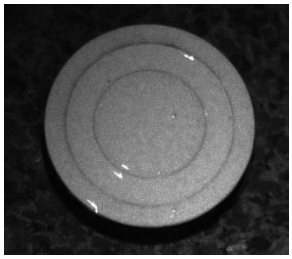

Figure 6. Speckle image captured with BASLER acA4096-30um camera

4.2 Speckle images captured with a smartphone

In all experiments with the portable laser and the smartphone sensor, the object was illuminated with red light. In this case, all necessary intensity information is contained in the red channel, therefore only the red channel of RGB images was analyzed during the postprocessing stage. The smartphone was connected to a PC as Wi-Fi and USB camera by iVCam software. Exemplary speckle images from the conducted experiments with resolution 1920×1080 and 3840×1020 are shown in Fig.7.

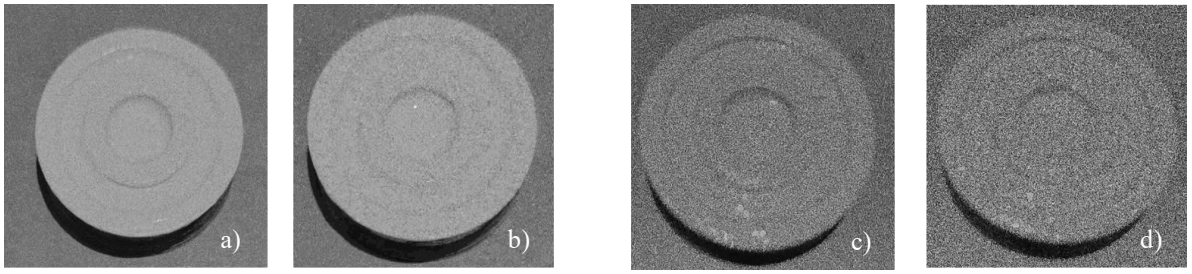

Figure 7. Speckle images captured with Xiaomi Mi9T camera connected to PC by: Wi-Fi with resolution 1920×1080 (a) and 3840×2160 (b); USB with resolution 1920×1080 (c) and 3840×2160 (d)

In the last set of experiments, images were captured with the smartphone's camera and stored directly in its memory. After the experiments, all data were transferred to the PC. In this case, we did not face reduction of image quality caused by application of iVCam software. As in previous experiments, images were captured in two resolutions.

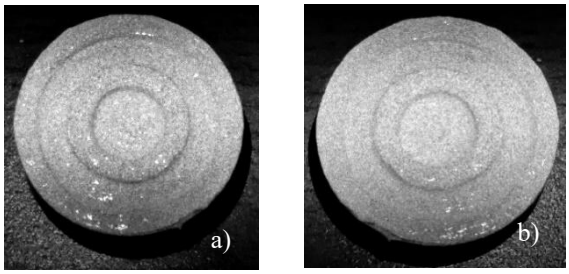

Figure 8. Speckle images captured with Xiaomi Mi9T camera. Data are stored in the smartphone's memory. Image resolution 1920×1080 (a) and 3840×2160 (b)

4.3 Activity maps

For each experiment, 10 activity maps were built with 200 speckle images acquired at time step 300 ms used to calculate each map. Therefore, one activity map shows the paint drying process per minute. To compare the results, we have chosen 3 activity maps related to the first, fifth and tenth minutes of the experiment. Below, Fig.9 shows the activity maps based on the ground truth speckle images. High contrast may be noticed on all of them.

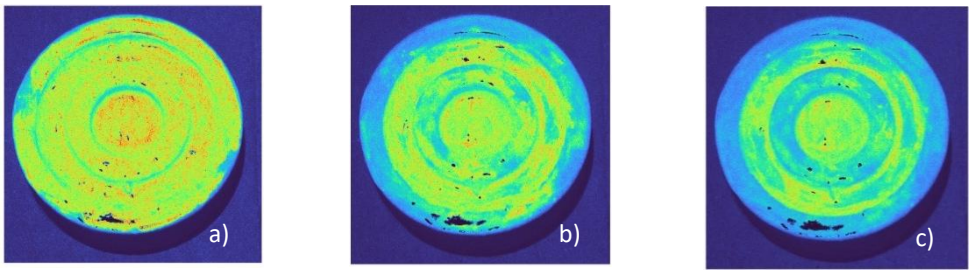

Figure 9. Activity maps based on original speckle images: a) 1st minute; 2) 5th minute 3) 10th minute.

Application of iVCam software reduces quality of the speckle images, thus influencing final quality of the activity maps (Fig.10). Quality is reduced because the captured images are compressed by JPEG standard at high compression level. Image degradation and artifacts caused by JPEG compression may be easily observed on the activity maps with resolution 1920x1080. Despite this visual drawback, JPEG standard does not critically change time correlation of speckle images[15] and even the low quality activity maps clearly show the change in activity during the experiment. It must be noted that for all sets of experiments, the time step was chosen equal to 300 ms since it determined the fastest rate at which the smartphone was able to transfer images at resolution 3840×2160 to the PC by Wi-Fi. In all other cases, images could be transferred faster.

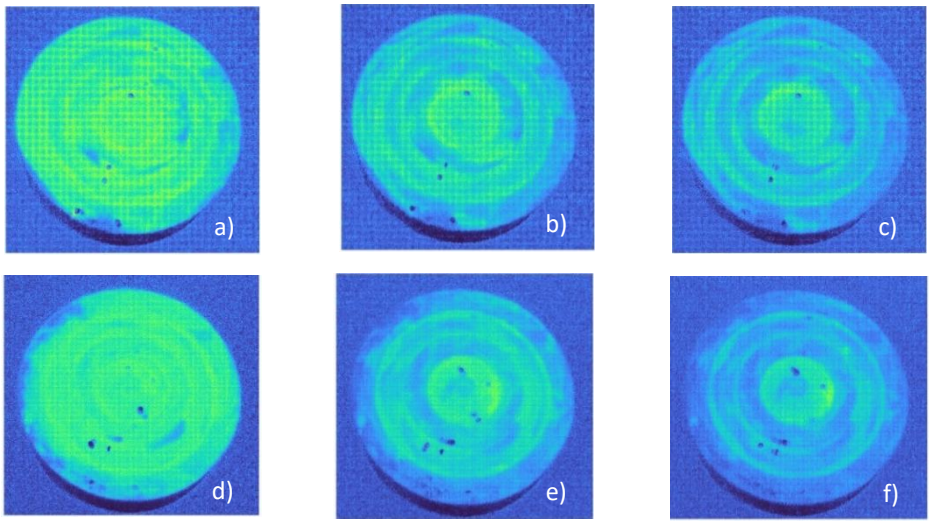

Figure 10. Activity maps based on speckle images captured with Xiaomi Mi9T camera connected to PC by Wi-Fi with resolution: 1920×1080 (a) (b) (c) and 3840×2160 (d) (e) (f); 1st minute – (a) (d); 5th minute – (b) (e); 10th minute – (c) (f).

In the next experiment, data were sent to the PC via USB cable (Fig.11). At resolution 1920×1080, the same image quality degradation and artifacts may be seen. Connection of the smartphone to PC via USB allows transferring images faster compared to the Wi-Fi case.

In both USB and Wi-Fi types of connection, the drying process can be clearly tracked. However, absolute values of the MSF estimate ~~algorithm~~ are less compared to the activity maps based on speckle images captured under laboratory conditions.

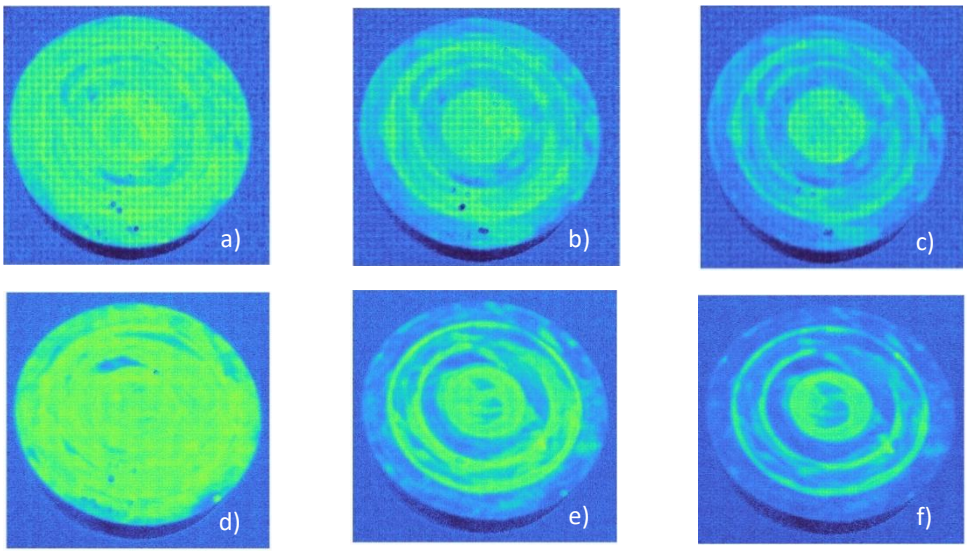

Figure 11. Activity maps based on speckle images captured with Xiaomi Mi9T camera connected to PC by USB with resolution: 1920x1080 (a) (b) (c) and 3840x2160 (d) (e) (f); 1st minute – (a) (d); 5th minute – (b) (e); 10th minute – (c) (f).

In the final experiment, the speckle images were captured and stored in the smartphone. After the experiment was finished, all images were transferred to the PC for processing. Some of the activity maps for the first, fifth and tenth minutes can be seen in Fig.12. The contrast of the maps obtained in the experiment is higher compared to the previous ones.

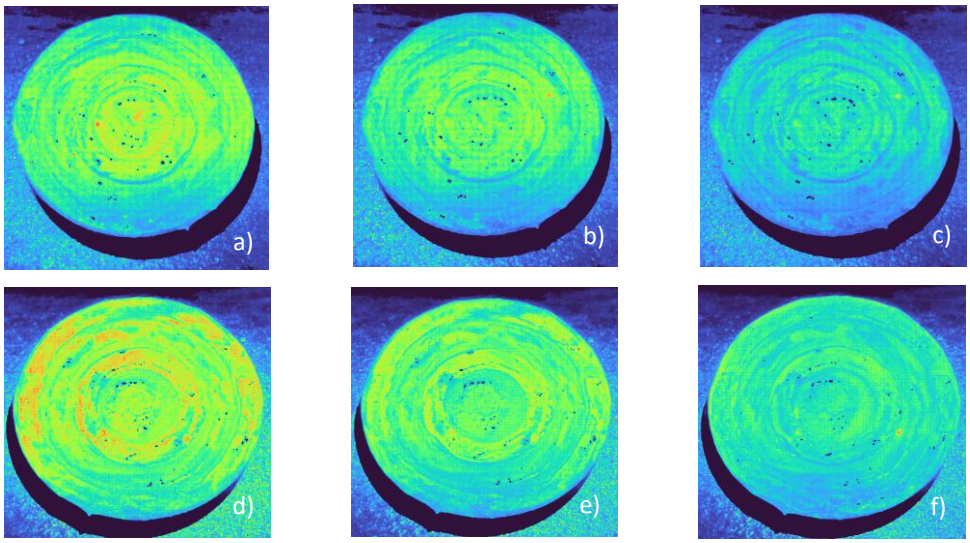

Figure 12. Activity maps based on speckle images captured with Xiaomi Mi9T with resolution: 1920×1080 (a) (b) (c) and 3840×2160 (d) (e) (f). Images are stored in smartphone's memory; 1st minute – (a) (d); 5th minute – (b) (e); 10th minute – (c) (f).

5. CONCLUSION

In summary, we proposed a low-cost portable setup for 2D intensity-based dynamic speckle technique. The input data for DST are correlated in time sequences of speckle images of an object's surface illuminated with laser. Images are captured with CCD or CMOS camera. The output of the method is a 2D activity map which shows speed of processes ongoing within the object. Most of the research experiments are carried out using expensive high-end equipment installed in laboratories, thus limiting the number of possible DST applications. The low-cost portable setup we proposed enables switching from laboratory to field conditions, substantially reduces price of the measurement and makes DST versatile and easily accessible for users.

In our research, we developed a laser device which was attached to the smartphone's case and carried out sets of experiments. As ground truth data, we considered speckle images captured in laboratory environment with high-end equipment and the built from them activity maps. For the low-cost setup, we used Xiaomi Mi 9T and a self-developed laser device to capture speckle images. The smartphone was connected to PC as i) IP-camera and ii) USB-camera. In the last experiment, speckle images were captured and stored in the smartphone's memory. We repeated each experiment twice at different image resolution: 1920x1080 and 3840x2160. Xiaomi Mi 9T was used as IP and USB camera by applying iVCam software. This software reduced quality of the speckle images and, hence, of the activity maps since the images were transferred being compressed with JPEG standard at low quality level. In addition, it was not possible to transfer data faster than 300 ms due to the smartphone's processor and Wi-Fi module limitations. The activity maps built from these images get artifacts, but nevertheless, they show the regions with different activity on the object's surface with satisfying quality. Best quality was achieved in the last set of experiments when the speckle images were captured and stored in the smartphone's memory. In addition, such type of data capturing is the fastest between the three types of connection which makes it suitable for detection of fast changing processes.

ACKNOWLEDGMENTS

This work was supported by Institute of Information & communications Technology Planning & Evaluation (IITP) grant funded by the Korea government (MSIT) (No. 2019-0-00001, Development of Holo-TV Core Technologies for Hologram Media Services). The research was done in the framework of COST Action CA21155 HISTRATE and related to it project КП-06-КОСТ/19 of Bulgarian National Science Fund. M. Levchenko thanks 2020 Plenoptic Imaging H2020 Marie Sklodowska-Curie Innovative Training Network, project No 956770. E. Stoykova thanks European Regional Development Fund within the Operational Programme "Science and Education for Smart Growth 2014–2020" under the Project CoE "National center of Mechatronics and Clean Technologies" BG05M2OP001-1.001-0008.

REFERENCES

[1] H. Fujii, K. Nohira, Y. Yamamoto, H. Ikawa, and T. Ohura, "Evaluation of blood flow by laser speckle imaging sensing Part I," Appl. Opt. 26(24), 5321–5325 (1987).

[2] A. Serov and T. Lasser, "High-speed laser Doppler perfusion imaging using an integrating CMOS image sensor," Opt. Express 13(17), 6416–6428 (2005).

[3] V. Rajan, B. Varghese, T. G. van Leeuwen, and W. Steenbergen, "Speckles in laser Doppler perfusion imaging," Opt. Lett. 31(4), 468–470 (2006)

[4] R. Braga, I. Fabbro, F. Borem, G. Rabelo, R. Arizaga, H. Rabal, and M.Trivi, "Assessment of seed viability by laser speckle technique," Biosystems Eng. 86(3), 287-294 (2003).

[5] R. Braga, G. Rabelo, L. Granato, E. Santos, J. Machado, R. Arizaga, H. Rabal, and M. Trivi, "Detection of fungi in beans by the laser biospeckle technique," Biosystems Eng. 91(4), 465-469 (2005).

[6] R. A. Braga, L. Dupuy, M. Pasqual, and R. R. Cardoso, "Live biospeckle laser imaging of root tissues," Eur. Biophys. J. 38(5), 679–686 (2009).

[7] B. Ivanov, E. Stoykova, N. Berberova, T.Nikova, E. Krumov, and N. Malinowski, "Dynamic speckle technique as a leaf contamination sensor", Bulg. Chem. Commun. 45(3), 149 – 153 (2013).

[8] E. Stoykova, B. Blagoeva, D. Nazarova, L. Nedelchev, T. Nikova, N. Berberova, Y. Kim, and H. Kang, "Evaluation of temporal scales of migration of cosmetic ingredients into the human skin by twodimensional dynamic speckle analysis," Opt. Quant.Electron. 50, 191-201 (2018).

[9] A. Chatterjee, P. Singh, V. Bhatia, and S. Prakash, "Ear biometrics recognition using laser biospeckled fringe projection profilometry," Opt. Las. Technol. 112, 368-378 (2019).

[10] S. E. Murialdo, G. H. Sendra, L. I. Passoni, R. Arizaga, J. F. Gonzalez, H. Rabal, and M. Trivi, "Analysis of bacterial chemotactic response using dynamic laser speckle," J. Biomed. Opt. 14(6), 064015 (2009). 11. B. Mandracchia, J. Palpacuer

[11] R. Macedo, J. Barreto Filho, R. Braga, Jr, and G. Rabelo, "Sperm motility decreasing and semen fertility in the bull evaluated by biospeckle," Reprod. Fertil. Dev. 22, 170–171 (2009).

[12] M. Z. Ansari, P. D. Minz, and A. K. Nirala, "Fruit quality evaluation using biospeckle techniques," in Proceedings of IEEE Conference on Recent Advances in Information Technology (IEEE, 2012) , 873–876.

[13] C. Mulone, N. Budini, F. Vincitorio, C. Freyre, A. López Díaz, and A. Ramil Rego,"Analysis of strawberry ripening by dyna

[14] R. Harizanova, V. Gaydarov, G. Zamfirova, E. Stoykova, D. Nazarova, B. Blagoeva, and L. Nedelchev, "Probing of the mechanical properties and monitoring of the drying process of azopolymer thin films for optical recording," Thin Solid Films 687, 137441 (2019).

[15] Stoykova, E., Blagoeva, B., Berberova-Buhova, N., Levchenko, M., Nazarova, D., Nedelchev, L., & Park, J. (2022). Intensity-based dynamic speckle method using JPEG and JPEG2000 compression. Applied Optics, 61(5), B287-B296.

Mikhail Levchenko, Elena Stoykova, Keehoon Hong, and Joongki Park "Portable low-cost setup for outdoor implementation of dynamic speckle technique", Proc. SPIE 12618, Optical Measurement Systems for Industrial Inspection XIII, 126181I (15 August 2023); https://doi.org/10.1117/12.2673460